# Spectral Analysis and POD of Turbulent Pipe

M. Raba

June 17, 2022

- Normalize pod modes (ok, debugging)
- Reynolds stress $u'u'$ (streamwise, before spectral analysis).
- Plot different $(k, m)$ (ok)
- Extract 2048 cs
  - need extract-slices-from-pipe-volume$_{v2.py}$, have only extract-slices-from-pipe-volume.py, how different?

## Normalize each POD mode as, $\int \Phi^H(r;m;k)\Phi(r;m;k)r\,dr$, where $r \in [0, 0.5]$.

```
vNormalize = zeros(ss,1);
for nm=1:ss
    pV = phiVec(podModeNumber).c(currentCrossSection).m(currentAzimuthalMode).dat(nm);
    vNormalize(nm)= rMat(nm)*ctranspose(pV)*pV;
end % nm
normRes = trapz(vNormalize,dr);
for nm=1:ss
    phiVecNormalized(podModeNumber).c(currentCrossSection).m(currentAzimuthalMode).dat(nm) =
↪   phiVec(podModeNumber).c(currentCrossSection).m(currentAzimuthalMode).dat(nm)/normRes;
end % nm x 2
end % podMode
```

## Plot different $(k, m)$

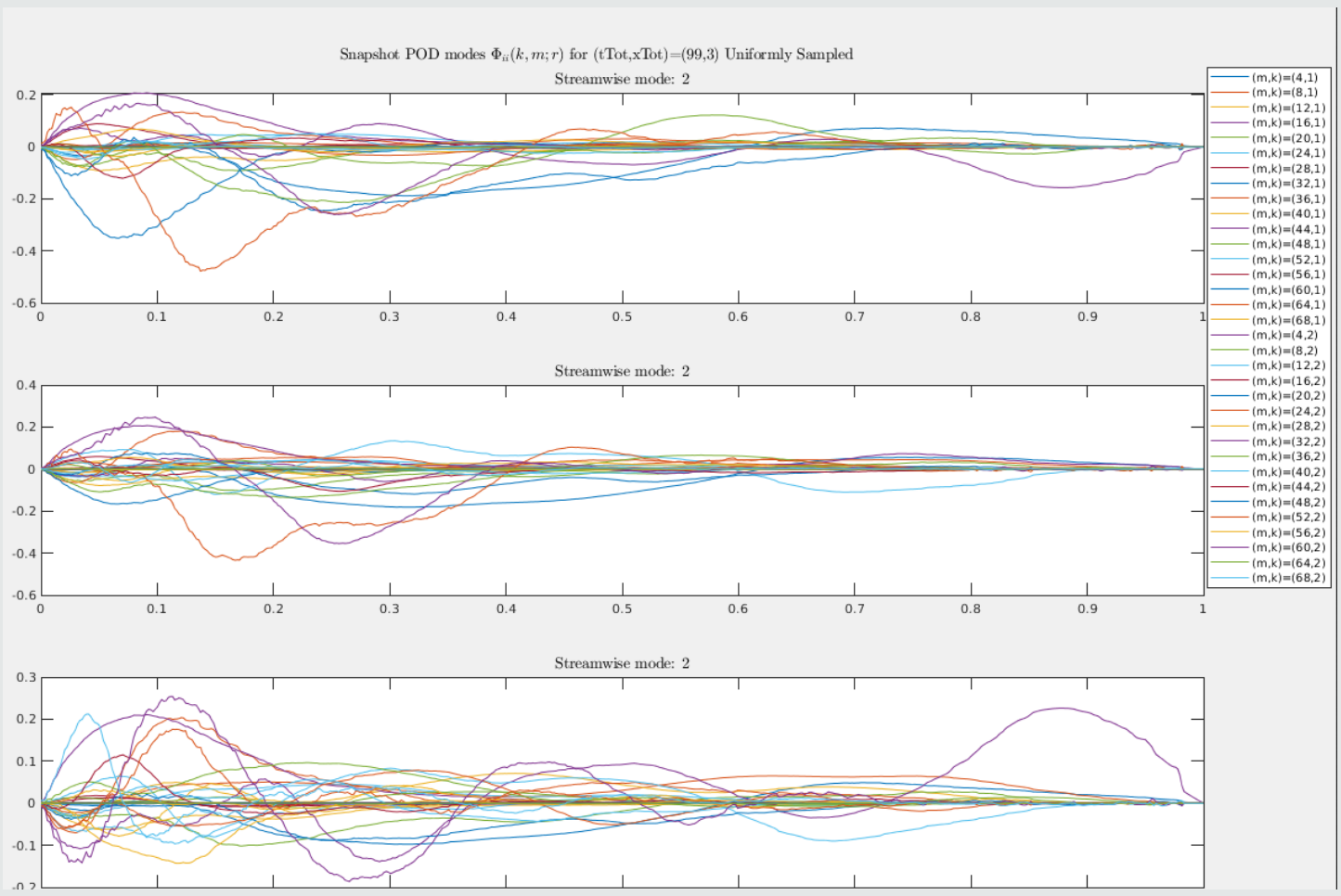


**Figure 1:** Snapshot Modes, Plotting different $(k, m)$ combinations. 99 evenly spaced snapshots, 3 crosssections; no normalization.

## Plot different $(k, m)$ with $\int u^H u r\,dr$ Normalization

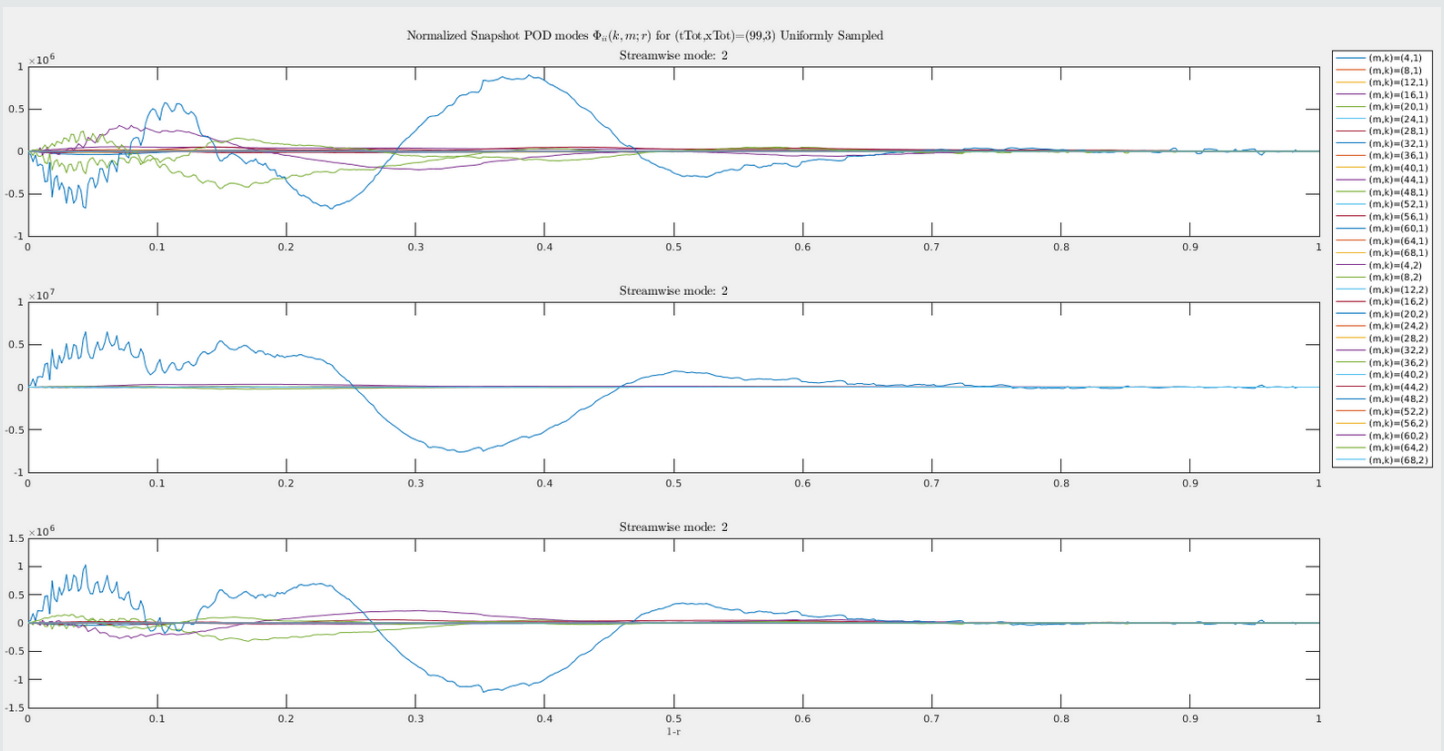


**Figure 2:** Snapshot Modes, Plotting different $(k, m)$ combinations. 99 evenly spaced snapshots, 3 crosssections; with Normalization **(under construction ! ! ! Obvious wrong plot, but verify the procedure)**

## Plot of Reynolds Shear $u'u'$ in Streamwise Direction

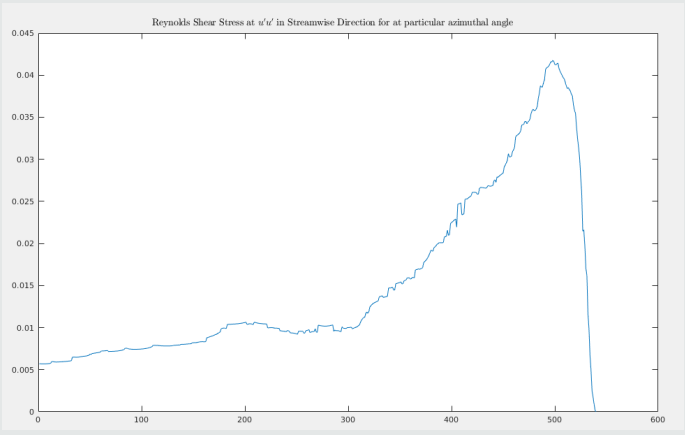


**Figure 3:** Plot of $u'u'$ at a particular azimuthal angle $\theta$

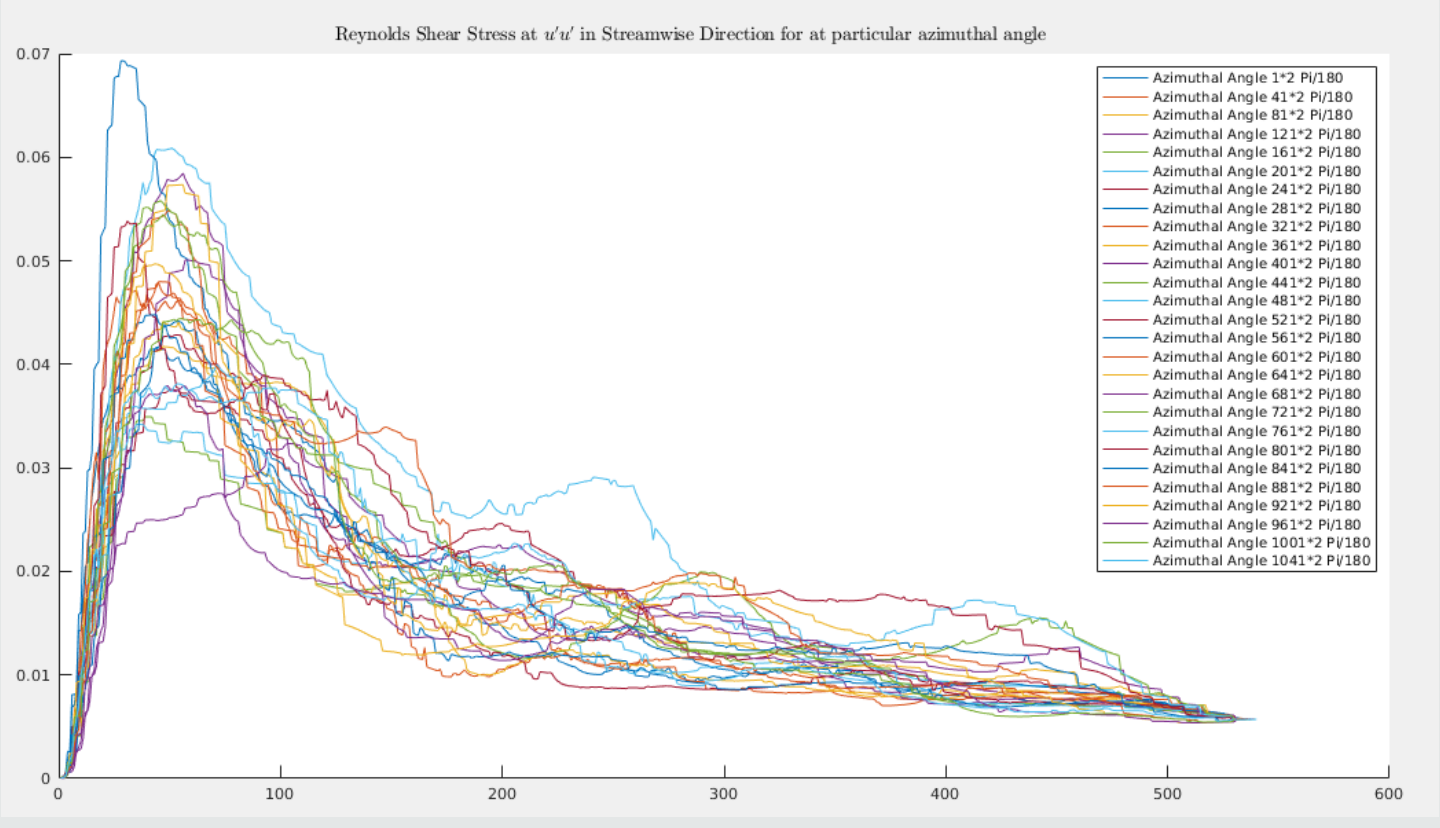


**Figure 4:** Plot of $u'u'$ at every 40th degree **for ntimesteps = 99**

## Needs to look similar to,

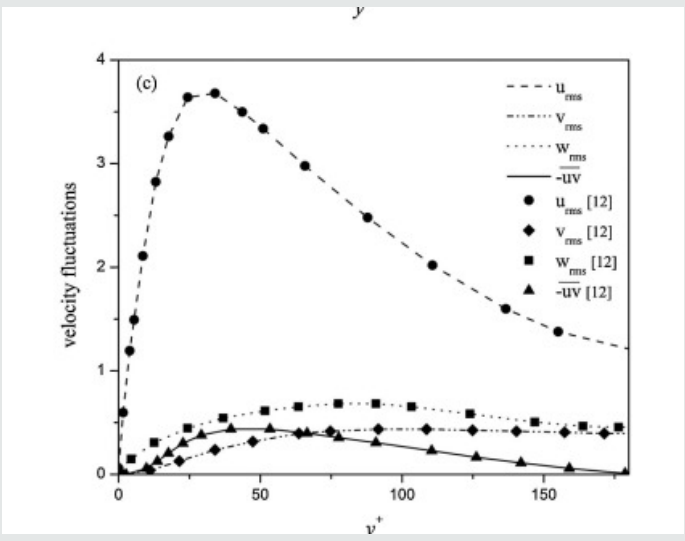


**Figure 5:** Needs to look like eg this, the tallest graph with amplitude ~ 3.

```
for mz=1:40:1080
uu=zeros(ss,1);
nts=ntimesteps
%for tt=1:ntimesteps
for tt=1:nts
for sz=1:ss
   uu = qMinusQbar_noCsYet(tt).circle(mz).dat(sz)  ;
   uuuz(tt).dat(sz) = uu*uu;
end  % sz
end % tt
rmsVec = zeros(ss,1);
for sp=1:ss
tVecc=zeros(nts,1);
for ts=1:nts
    thVec(ts) = uuuz(ts).dat(sp);
end
daRoot = rms(thVec);
rmsVec(sp) = daRoot;
end
labelStr = ['Azimuthal Angle ' num2str(mz) '*2 Pi/180']
hold on
plot(flip(rmsVec),"DisplayName", labelStr)
```

## Smits 2014. Phase Shifting

### III. SNAPSHOT POD ANALYSIS

Figure 1 shows the scaled energy contribution of the first 30 sPOD modes for both Reynolds numbers. The modal energy is distributed over a large number of modes, and the modes appear to occur in pairs with similar energy content. The first 10 sPOD modes represent 14% and 15% of the energy for $Re_D = 47{,}000$ and 93,000, respectively. The modal energy distribution reported by Hellström *et al.*[11] for $Re_D = 12{,}500$ shows a similar behavior, in that the first 10 modes contained 14.5% of the energy, and some modal pairs were observed. However, the relatively short temporal window explored in that study (equivalent to about $20R$ in length) led to some inconsistencies. For instance, the modal shape of the first sPOD mode in that study is similar to that of modes 5 and 6 in the present study, suggesting that the energy for the first mode was overrepresented.

In the present results, the energy distribution and the modal shape changed little in going from $Re_D = 47{,}000$ to 93,000, and only the higher Reynolds number is considered for the remainder of this section.

The first six sPOD mode shapes are shown in Figure 2. The modes making up the first energy pair (sPOD modes 1 and 2) are obviously the same azimuthal mode with mode number $m = 3$, but azimuthally phase shifted by $\pi/6$, enforcing the orthogonality. Similarly, the second pair (sPOD modes 3 and 4) represents $m = 2$, and the third pair (sPOD modes 5 and 6) represents $m = 4$, where the azimuthal phase shifts between the members of a pair are given by $\pi/(2m)$.

The structures within each mode in Figure 2 extend from the wall well into the central part of the pipe, corresponding to the wake region in the mean velocity profile. These structures are very

Figure 6: Description from hellstrom2015 About Phase Shifting. This could be used to get the different peaks for each $m$ in the below graph.

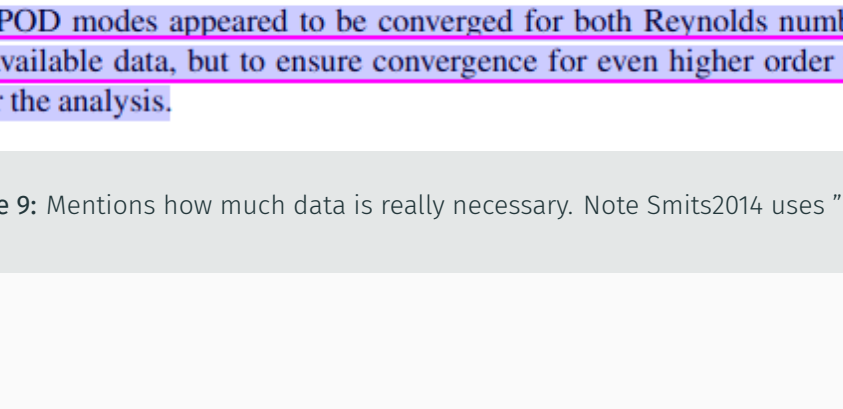


Figure 7: Leo2015 paper. Graph of classical POD. The radial behavior of the cPOD modes. (a) Azimuthal modes $m = 1 - 10$ for the first cPOD mode, $n = 1$. − − −, $\mathrm{Re}_D = 47{,}000$; — $\mathrm{Re}_D = 93{,}000$. (b) cPOD modes $n = 1 - 3$ for $m = 3$, where $n = 1, 2, 3$ is represented by − − −, and ⋯, respectively; using (classical) eigenproblem $\int_{r'} \hat{S}_{ij}(r, r'; m; f)\, \hat{\phi}_j^{\circ(n)}(r'; m; f)\, dr' = \hat{\lambda}^{(n)}(m; f)\hat{\phi}_i^{(n)}(r; m; f)$.

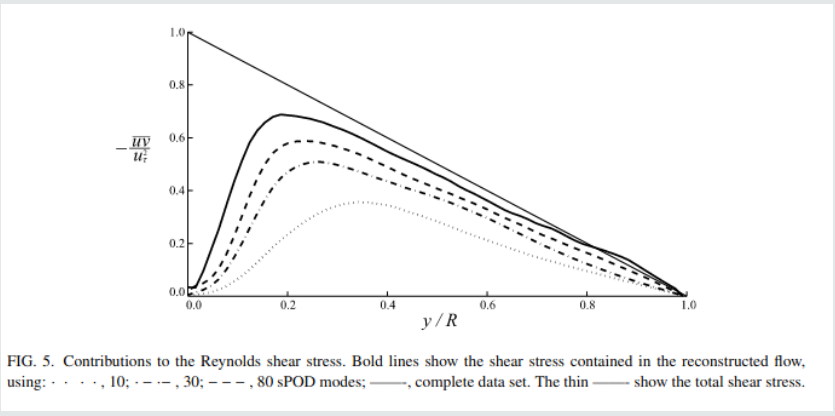


FIG. 5. Contributions to the Reynolds shear stress. Bold lines show the shear stress contained in the reconstructed flow, using: · · · ·, 10; · − ·−, 30; − − −, 80 sPOD modes; ——, complete data set. The thin —— show the total shear stress.

Figure 8: The Reynolds shear stress for the above cPOD.

## Smits2014 Convergence

In Smits2014, their classical POD problem uses a single crosssection, and instead of fft over cs, they fft in time, so their kernel is the doubly Fourier-transformed velocity fluctuation $\hat{S}$, cross-spectral Matrix.

$$\int_{r'} \hat{S}_{ij}(r, r'; m; f)\, \hat{\phi}_j^{((n)}(r'; m; f)\, dr' = \hat{\lambda}^{(n)}(m; f)\hat{\phi}_i^{(n)}(r; m; f) \tag{1}$$

Snapshot and classical POD (from here on referred to as sPOD and cPOD, respectively) were performed on the three-component fluctuating velocity data, which consisted of 22, 210 snapshots divided into ten blocks. Since both sPOD and cPOD were performed in pipe coordinates, each velocity component was multiplied by $\sqrt{r}$ to make the kernel Hermitian symmetric.[4,24] For snapshot POD, the first ten sPOD modes appeared to be converged for both Reynolds numbers after using only 1/10th of the available data, but to ensure convergence for even higher order modes, the full data set was used for the analysis.

Figure 9: Mentions how much data is really necessary. Note Smits2014 uses ” POD.

## Smits, Ganapathisubramani, Hellstorm 2015

Follows Citrini and George Procedure (twice cross-spectral matrix), the following graphs are found

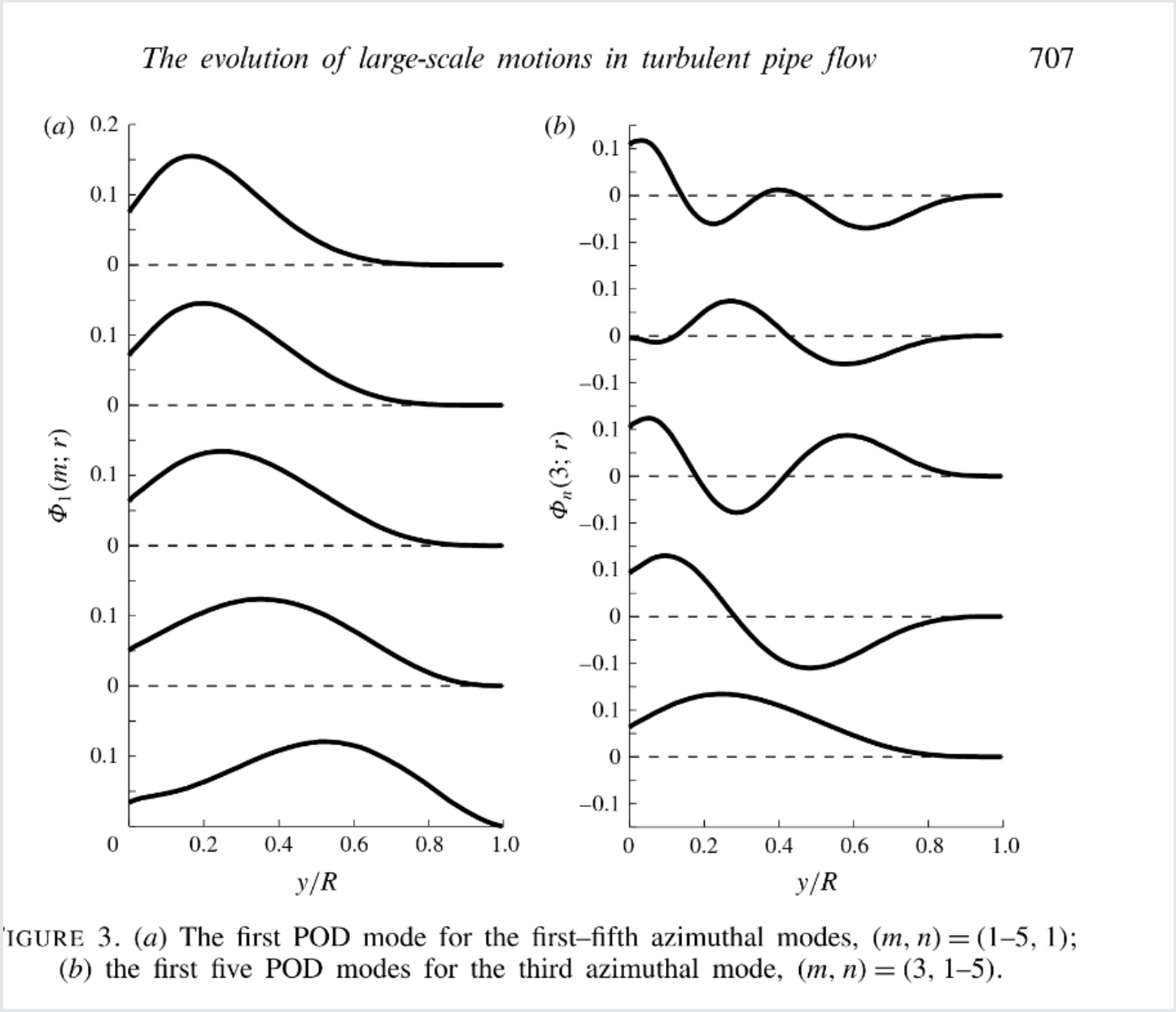


FIGURE 3. (a) The first POD mode for the first–fifth azimuthal modes, $(m, n) = (1–5, 1)$; (b) the first five POD modes for the third azimuthal mode, $(m, n) = (3, 1–5)$.

Figure 10: Moving to a different paper, this time Hellstrom, Ganapathisubramani and Smits 2015. Displays higher POD modes in combination with $m$. Note, follows Citrini and Georg's Procedure with $S(m; r, r') = \lim_{\tau\to\infty} \frac{1}{\tau} \int_0^\tau r^{1/2} u(m; r, t) u^*(m; r', t)\, r'^{1/2}\, \mathrm{d}t$ and $\lim_{\tau\to\infty} \frac{1}{\tau} \int_0^\tau r^{1/2} u(m; r, t) \alpha_n^*(m; t) \mathrm{d}t = \Phi_n(m; r) \lambda^n(m)$

## Smits, Ganapathisubramani, Hellstorm 2015 (PIV Data Capturing Frequency)

- Frequency

The three 5.5 Megapixel LaVision Imager sCMOS cameras were operated at 30 Hz with an interframe time of 40 μs, so that at $Re_D = 104\,000$ there was a bulk convective displacement of $0.96R$ between two consecutive data planes. The flow was seeded using 10 μm hollow glass spheres, and although the scattered light lost some of its polarization, the polarization was sufficient to separate the two orthogonal images with little cross-talk.

The test section was enclosed by an acrylic box, filled with water to minimize the optical distortion due to refraction through the pipe wall. The pipe wall thickness ($1.27 \pm 0.064$ mm) was minimized to further reduce the reflection and distortion caused by the mismatch between the refractive index of water and that of glass. The PIV calibration method was similar to that presented by van Doorne & Westerweel (2007) and Hellström *et al.* (2011). An access port was located immediately downstream of the test section in order to insert the planar and stereo PIV calibration targets while the pipe was filled with water. The stereo PIV target was a 1.6 mm thick plate with 272 dots set in a rectangular grid. The target was traversed 2 mm in each direction of the laser sheet, resulting in three calibration images for each stereo PIV camera. The planar target was a 150 mm long D-shaped cylinder having circular ends, with 189 dots arranged in a rectangular grid. The target was attached to a micrometer stage for streamwise alignment of the streamwise plane with the cross-plane.

Figure 11: frequency

## Smits, Ganapathisubramani, Hellstorm 2015 (Singularity Avoidance! and Gridpoints Data)

The data consisted of ten blocks, each containing 2200 image pairs. The images were processed using DaVis 8.1.6, and the resulting velocity field for the cross-plane consisted of 20 vectors $\mathrm{mm}^{-2}$ on a square mesh. The velocity components were interpolated onto a new mesh with polar coordinates $[r, \theta, x]$, having 132 radial mesh points spaced a distance $\Delta r$, and 834 azimuthal mesh points, matching the vector density at the wall while oversampling at the pipe centre. The streamwise plane resulted in 15 vectors $\mathrm{mm}^{-2}$, and these data were interpolated onto a mesh with radial grid points that matched the cross-plane. The singularity point at $r = 0$, when performing POD, was avoided by offsetting the inner mesh points by $\Delta r/2$.

In the streamwise plane approximately 100 vectors, corresponding to 0.3 % of the total vector count, were corrupted by the depolarized scatter off the pipe wall from the cross-plane light sheet. These vectors were estimated by performing snapshot POD on the streamwise plane, while excluding the corrupt vectors. The excluded vectors were then interpolated for each snapshot POD mode, where the fields are smoother than in the instantaneous velocity realizations. The complete velocity field was subsequently obtained by reconstructing the interpolated POD modes.

Figure 12: **Avoiding singularity in calculating POD** when doing $\Phi = r^{-1/2}\hat{\Phi}$ final recovery calculation.

## Question:

- In Smits2017, where the crossspectra is streamwise, that the flow is stationary and homogeneous in $x$ direction. Is this true from a rotating pipe flow?
  - If not, an alternative is to fft in $t$ as in Smits2014.

## Two POD approaches

- **Two branches of code**: snapshot pod and classic pod. Follow Smits2017
  - Both have switches for direct mutliply for correlation.

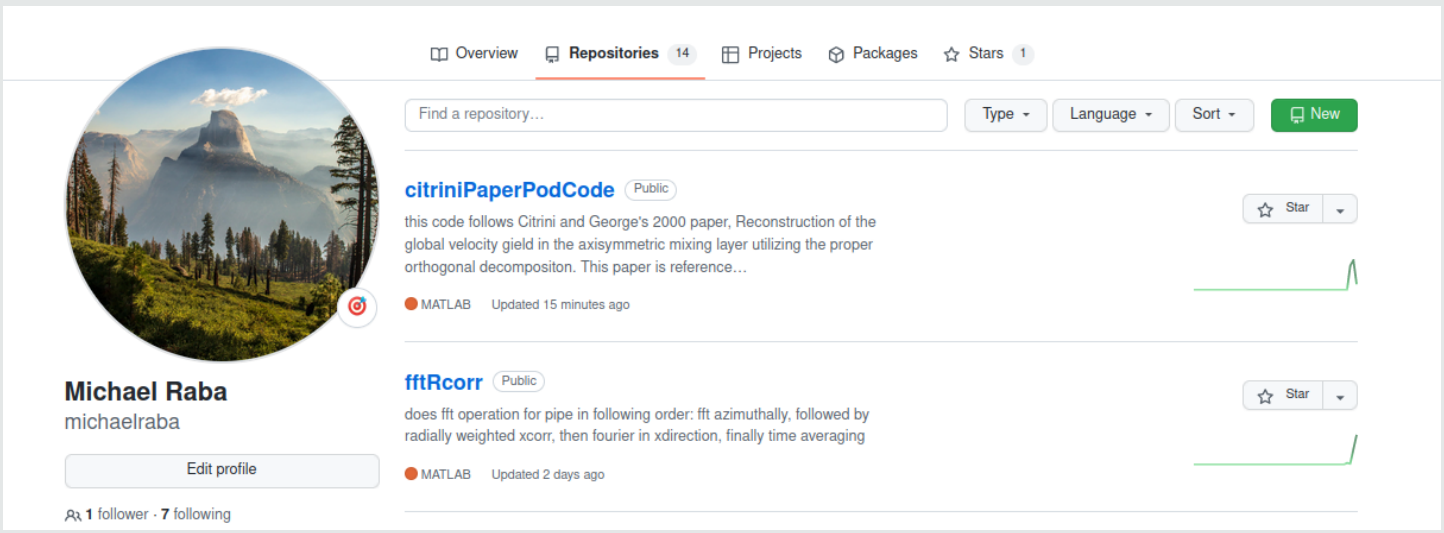


Figure 13: Snapshot and Classic POD Codes

## Snapshot

- branch Snap.A. fft-th->xcorr(t,t')->fft(x)
- branch Snap.B. fft-th->fft(x)->correlate via direct mult->average in time
- pod via following eq 2.4 and then 2.5.

## Classic

- branch A. fft-th->xcorr(x,x')->fft(x)
- branch b. fft-th->direct mult corr->fft(x)
- pod follows equation 2.1
- Snapshot is only more expedient if using full velocity components spectral density matrix. Otherwise that has greatly more steps for getting the pod modes.
  - the problem is not $3r \times 3r$ transformed to $t\times$.
- **Snapshot procedure**: form correlation $\mathbf{R}(k;m;t,t') = \int_r \mathbf{u}(k;m;r,t)\mathbf{u}^*(k;m;r,t')\,r\,\mathrm{d}r$ ; then solve 2.4 for $\alpha^{(n)}$, then solve 2.4 for $\Phi_T^{(n)}$.
- **Classic POD**: form correlation $\mathbf{S}(k;m;r,r') = \lim_{\tau\to\infty}\frac{1}{\tau}\int_0^\tau \mathbf{u}(k;m;r,t)\mathbf{u}^*(k;m;r',t)\,\mathrm{d}t$; Just do SVD/eig solve;

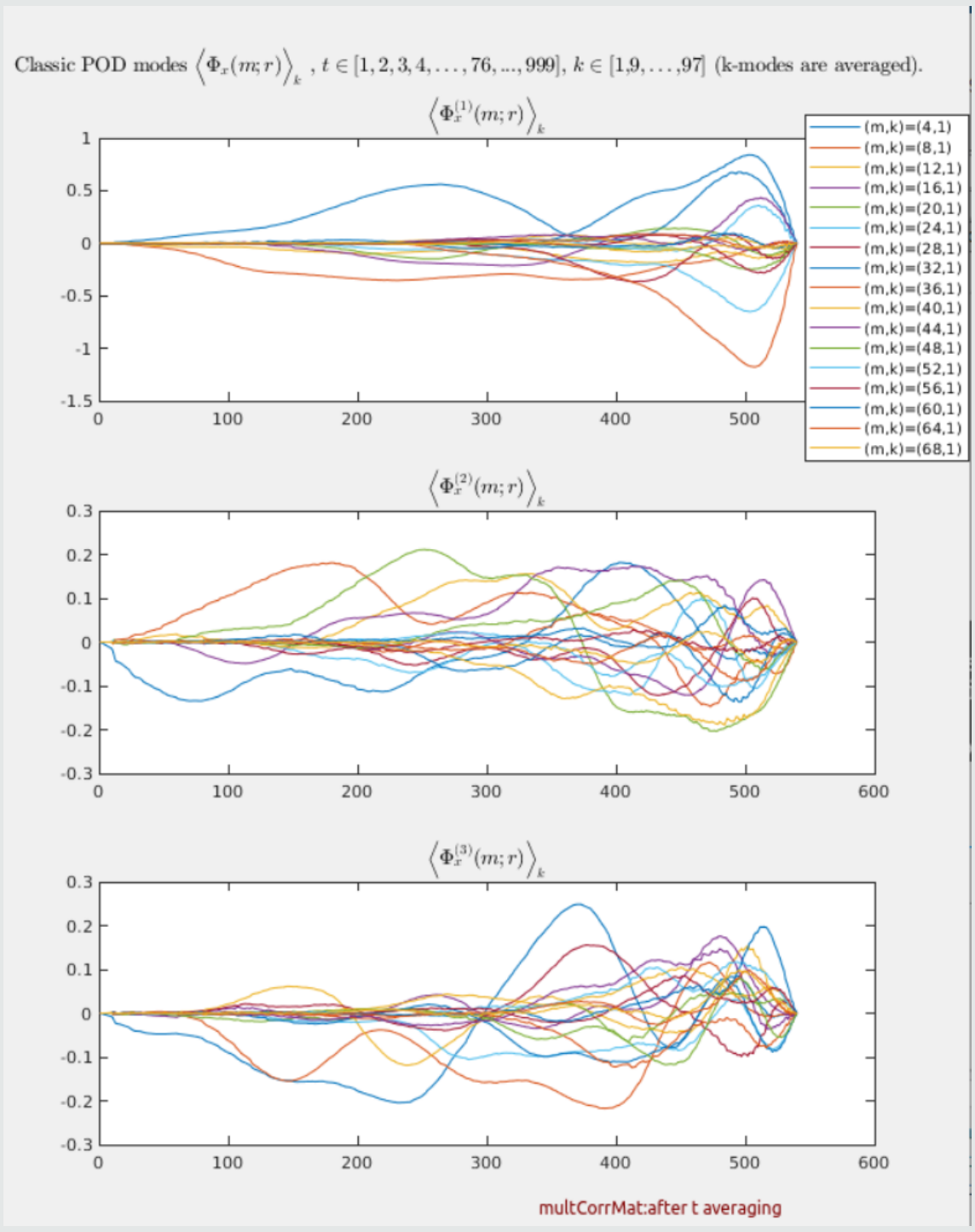


Figure 14: Classic POD Modes closely following Smits2017 procedure (direct mult used); medium size run (full time step and every 9th crosssection); link to .Mat file

## Worry about Convergence of streamwise FFT

- Zigunov's advice:
  - we need long time series to get converged statistics (say, for example in the case of Fourier Analysis of V, we need as many entries in V as possible). This is particularly the case in experiments, where noise can contaminate the spectrum and spectral averaging can "clean up" our data by a good amount.
  - In general, Fourier analysis needs long data sets to capture periodicity with a good amount of certainty.
  - Upshot: need to show fft(x) is actually converged by varying density of crosssections. If not, more cs necessary !

## Smits 2017 used Such a large streamwise resolution:

### 2. Proper orthogonal decomposition

Here, we use 600 DNS data blocks for $Re_D = 24\,580$, acquired by Wu *et al.* [34], where each block domain is $30R$ long with a grid resolution $[r, \theta, x] = [256, 1024, 2048]$, with a streamwise periodic boundary condition. The blocks are acquired every $100\,\Delta t$, corresponding to a convective bulk flow displacement of $0.9R$. Additional details of the simulation are given by Wu & Moin [10].

Figure 15: Smits2017 data resolution. This shows 2048 crosssections were used. That was perhaps necessary to achieve convergence in the fft streamwise. In order to show that is indeed not necessary, a convergence study must be done

## Then they saved a fraction of that to file.

### 3. Discussion

The POD modes are insensitive to the streamwise mode number, and we will therefore present the energy as integrated over all $k$. The POD analysis is truncated due to the large amount of data and is resolved up to $[\pm k, m, n] = [2 \times 128, 64, 256]$, corresponding to azimuthal and streamwise wavelengths $\lambda_\theta/R = 0.098$ and $\lambda_x/R = 0.234$. These resolved modes capture 95.4% of the total turbulent kinetic energy. The relative kinetic energies for each of the first five POD modes and first 20 azimuthal modes are shown in figure 4.

Figure 16: Smits2017 data resolution. This shows that 128 streamwise modes were then saved to file and averaged. But 2048 crosssections were initially processed.

## Not necessary?

- Then show that with actual convergence study.
- Also compare with more papers.

## Goal Project resolution (viz: finish Msc)

- If this data set is too large, then cannot replicate Smits' result.
- a valid procedure has been developed, other phyiscs can be gleaned by smaller data sets
- Downside of this project: lot of data, perhaps intractable for a short term project
  - Lot of unneceessary uncertainty introduced by predecessor's results (lack of version control, no record of code's output, code needs to be documented to a higher standard: no intermediate results and incomplete procedure).

## Timeline A of Project conclusion (+)

- Expected Time to get more crosssecion data I dont have a good estimate for that. If one expects Smits2017 results then one needs $2048 \times ntimesteps$.
  - Tecplot did not seem to extract that data in a parallel way, even when parallel was called.
- Finish December Would be able to get paper but requires a bit more time

## Timeline B of Project conclusion (-)

- work with current data
- do spectral analysis on limited data, but won't be able to get results for JFM paper
- This is not desirable
- Finish at end of Summer. No paper but just get done. Scope of project was overestimated.

## Done A: Snapshot POD

- Correlation matrix is computed two ways (switch implemented for this)
  - A) either using xcorr (form assuming stationary and ergodic hypothesis, see below pages for that explanation)
  - B) direct calculation.
- Graph of classic POD run — looks rough

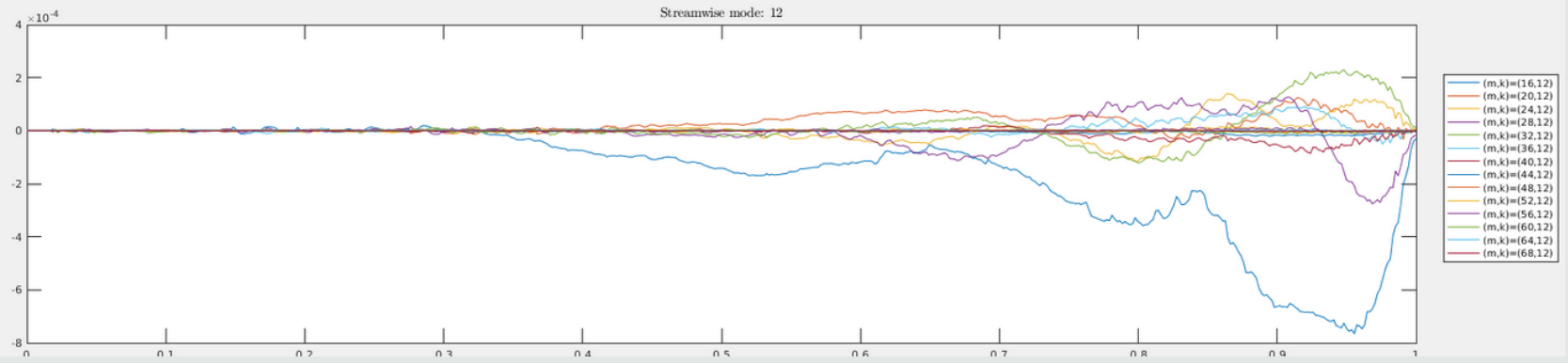


**Figure 17: snapshot pod run** update this.

- I'm thinkign that this can be better resovled if the temporal correlation is completely uncorrelated (this is the opposite of classic pod, where we want the correlation in radial)
  - papers say something ot this effect (add).

## Done B: Classic POD, Large run done.

- change fft($\theta$) to fourier($\theta$) ( function *fourier2.m* )
- Large run is all timesteps, 1/2 of the crosssection
  - runtime: ~13 hours ∴ code is parallized and does fourier($\theta$) first.

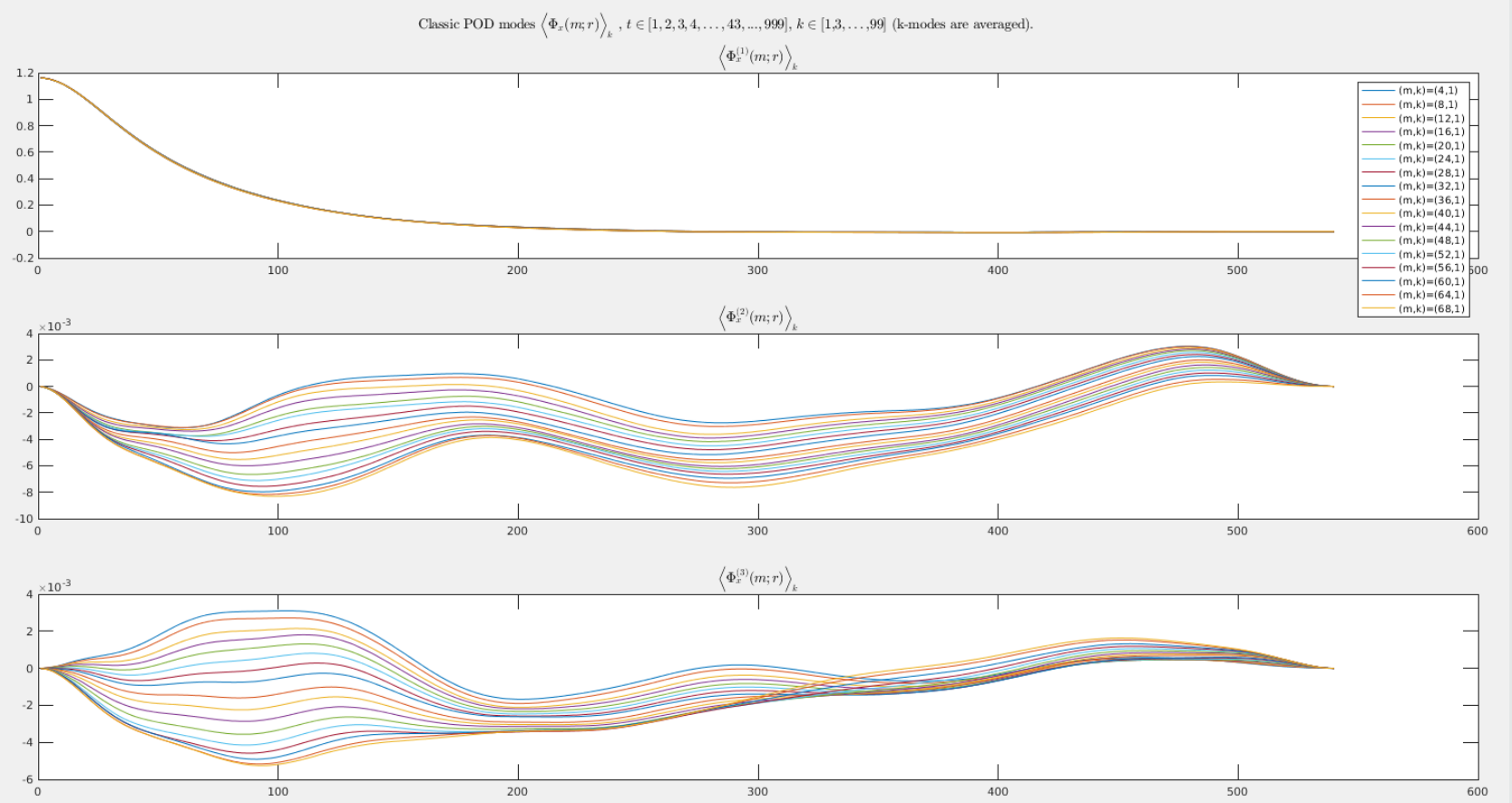


**Figure 18:** *classic pod run1 sized run (not a lot of crosssections used):

## Need to do:

- Classic POD, with **full components**: $u, v, w$ correlation matrix ...currently, just using streamwise component.
  - Needs a switch for direct correlation matrix calc. Cannot use xcorr for this as can be done for time-correlation (because not homogeneous/stationary in the radial direction.)
    - nb need to extract full interpolated components to disk ~ 5 TB.
- **Answer Major question:** Should we have correlation in time at all?
  - Tentative answer: **No. velocity fluctuations should have no time correlation at all, and any spikes in the time correlation would effect the POD graph (make it look like aliasing occurs)**.
    - **Idea:** by increasing timestep, that can decrease correlation , and therefore make the spectral analysis result less jittery.

## Reminder of Goal: reconstruct the following

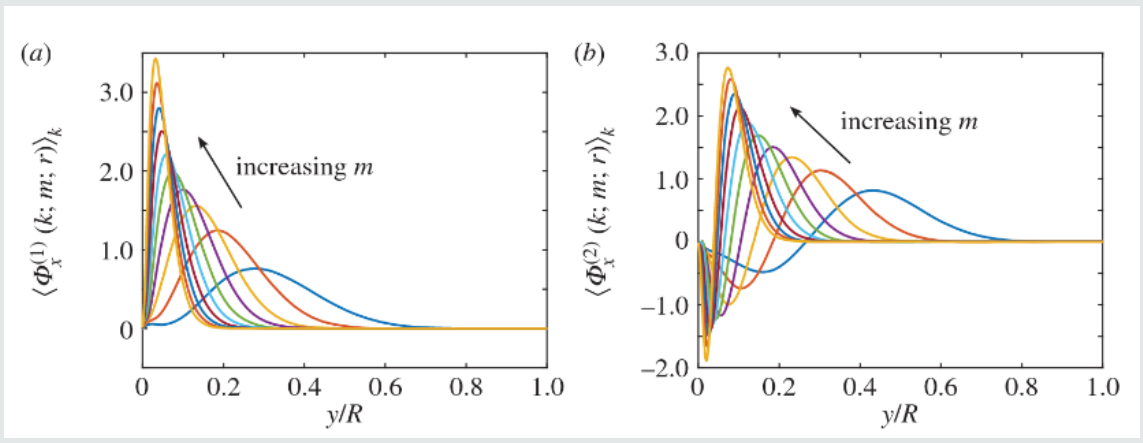


**Figure 19:** Smits 2017

## Classic POD ⇝

- Radial Correlation — for antipating Classic POD Result (show graph:)

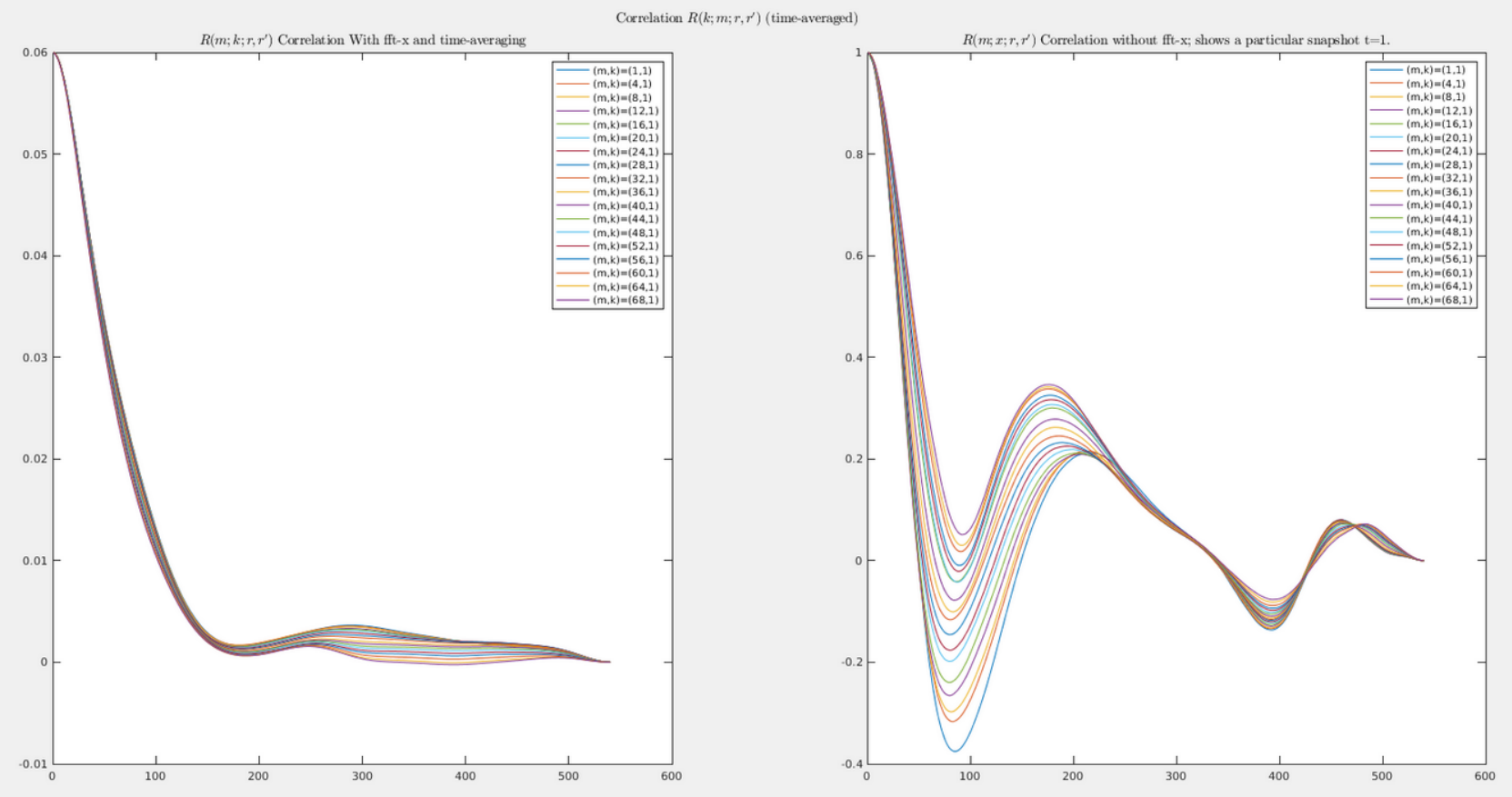


**Figure 20: Radial Correlation. left** After applying fft in x-dir. **Right:** no fft-x applied yet (just fft-$\theta$ and correlating).

- Compare to graphs of correlation data from eg Eggels et al

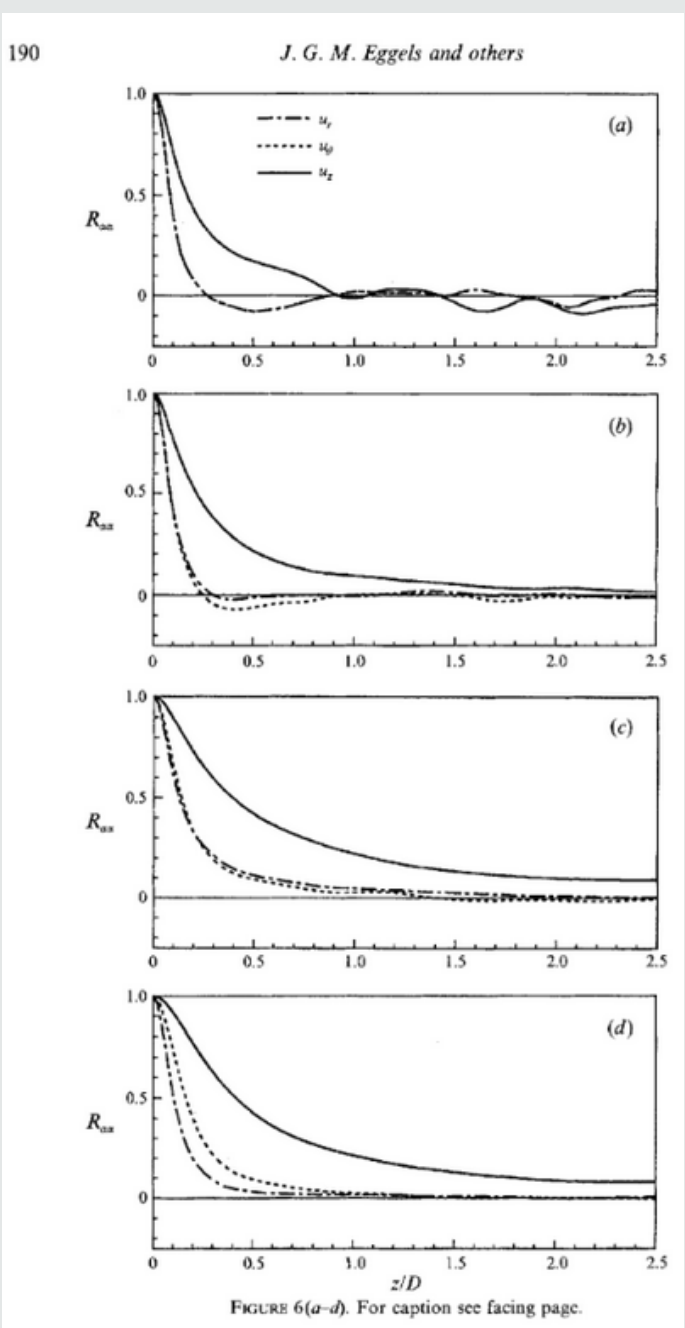


**Figure 21: Eggels et al Correlation, FigURe 6.** Two-point correlation coefficients of the thrce fluctuating velocity components computed from the DNS(E) data as functions of the streamwise separation distance $z/D$ : $(a) r/D = 0.008$, $y^+ = 177.2$; $(b) r/D = 0.247, y^+ = 90.9$; $(c) r/D = 0.451, y^+ = 17.8$; $(d) r/D = 0.487, y^+ = 4.7$

## Classic correlation matrix Formation

- Form symmetric positive definite matrix.

$$S(r,r';m;k) = \begin{bmatrix} u(0)u^H(0) & u(0)u^H(1) & u(0)u^H(2) & \dots & u(0)u^H(R) \\ u(1)u^H(0) & u(1)u^H(1) & u(1)u^H(2) & \dots & u(1)u^H(R) \\ \vdots & & & & \\ u(m)u^H(0) & u(m)u^H(1) & u(m)u^H(2) & \dots & u(m)u^H(R) \end{bmatrix} \tag{2}$$

- The matrix needs to be formed with $u, v, w$ components, which are stacked as , eg for 2d, Wu Kuisheng (2018) do:

$$U = \begin{bmatrix} u_1(x_1) & u_2(x_1) & \cdots & u_N(x_1) \\ u_1(x_2) & u_2(x_2) & \cdots & u_N(x_2) \\ \cdot & \cdot & \cdot & \cdot \\ u_1(x_M) & u_2(x_M) & \cdots & u_N(x_M) \\ v_1(x_1) & v_2(x_1) & \cdots & v_N(x_1) \\ v_1(x_2) & v_2(x_2) & \cdots & v_N(x_2) \\ \cdot & \cdot & \cdot & \cdot \\ \cdot & \cdot & \cdots & \cdot \\ v_1(x_M) & v_2(x_M) & \cdots & v_N(x_M) \\ \cdot & \cdot & \cdot & \cdot \\ w_1(x_1) & w_2(x_1) & \cdots & w_N(x_1) \\ w_1(x_2) & w_2(x_2) & \cdots & w_N(x_2) \end{bmatrix} \tag{3}$$

- Then correlation matrix $\mathbf{C}$ to describe the temporal correlation of flow field is $\mathbf{C} = \frac{1}{N}\mathbf{U}^H\mathbf{U}$.
- In particular, in contast to snapshot POD, we need to form the correlation matrix with all 3 flow field components;
- **Compare with snapshot pod**. That is why snapshot pod is more efficient. we just need to find correlation matrix in time, so dont have component for $u, v, w$, just would have $t$. Then the streamwise POD mode $\alpha^{(n)}$ is found as a projection onto $w$, the streamwise component.

## Snapshot POD

- Forming the temporal correlation tensor, for statistically stationary data, we can write the correlation matrix as,

$\rightsquigarrow$

$$S(r, r'; m; k) = \begin{bmatrix} u(0)u^H(0) & u(0)u^H(1) & u(0)u^H(2) & \dots & u(0)u^H(m) \\ u(1)u^H(0) & u(1)u^H(1) & u(1)u^H(2) & \dots & u(1)u^H(m) \\ \vdots & & & & \\ u(m)u^H(0) & u(m)u^H(1) & u(m)u^H(2) & \dots & u(m)u^H(m) \end{bmatrix} \tag{4}$$

- Since assumed homogeneity and statistically stationary and ergodic signal,

$$S(t, t'; m; k) = \begin{bmatrix} S(0) & S(1) & S(2) & \dots & S(m) \\ S(1) & S(0) & S(1) & \dots & S(m-1) \\ S(2) & S(1) & S(0) & \dots & S(m-2) \\ \vdots & & & & \\ S(m) & S(m-1) & S(m-2) & \dots & S(0) \end{bmatrix} \tag{5}$$

- Snapshot correlation Result:

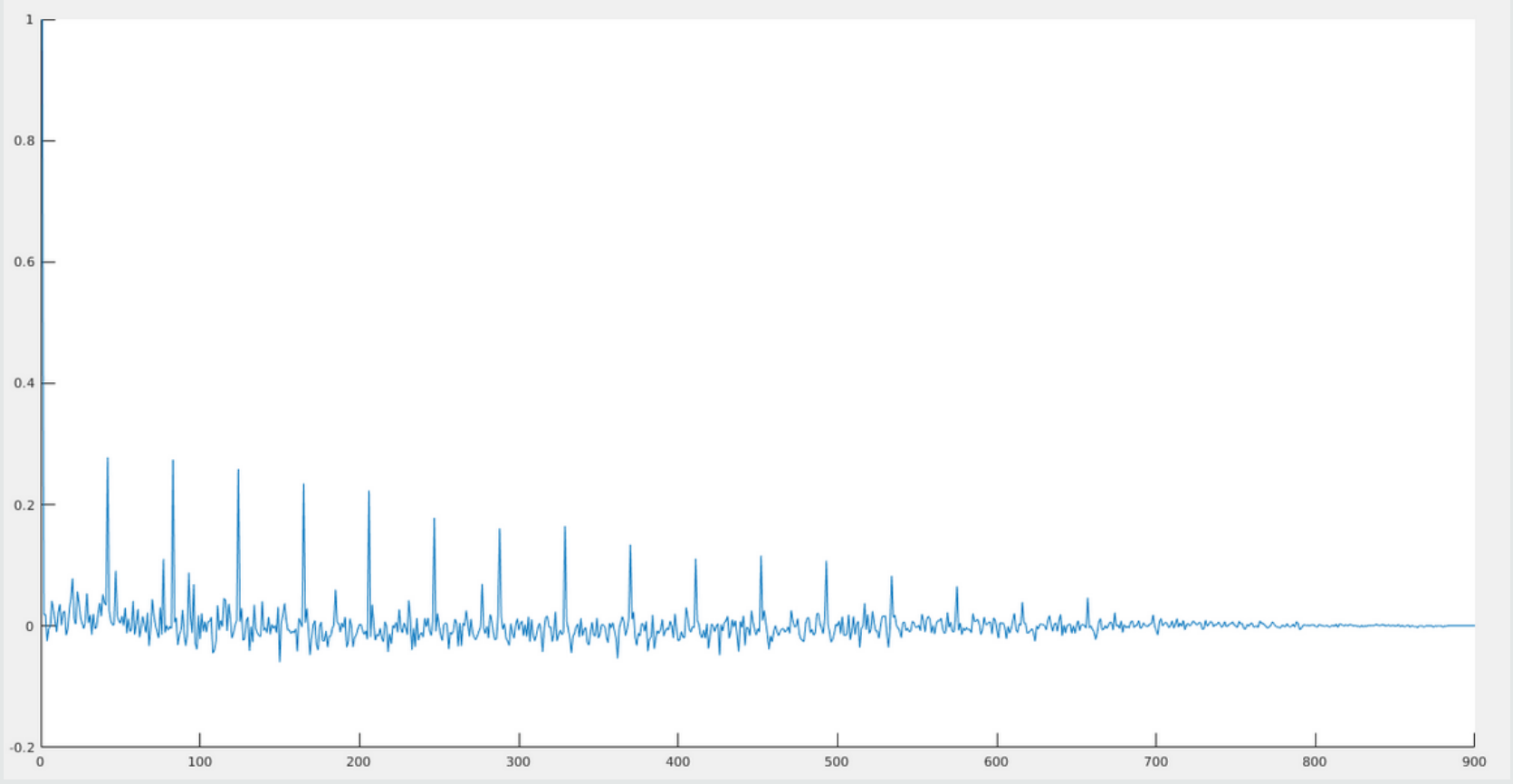


**Figure 22: Temporal Correlation.** Result of fft-$\theta$ then forming the correlation matrix. The graph is a row of that matrix, ie $\{S(0), S(1), S(2), \dots, S(m)\}$, where $S(t_i)$ is the correlation at various lags $t_i$.

- either too periodic (correlated) or not smooth enough (no correlation)
  - according to (source) $\alpha^{(n)}$ should be totally uncorrealted.

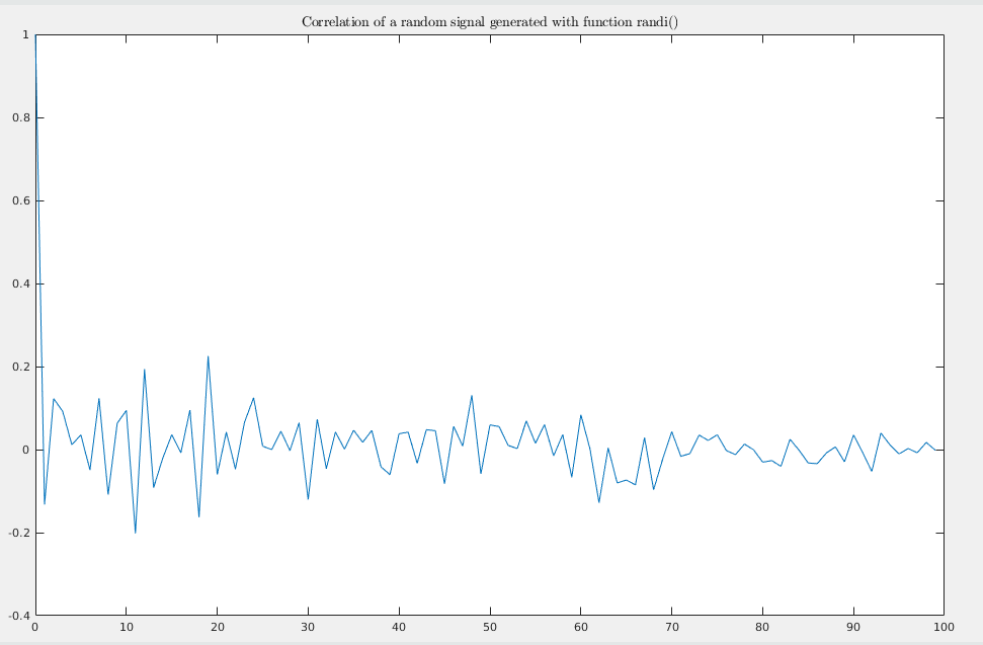


**Figure 23: Correlation of random signal.** In order to smooth out our signal, the temporal correlation ought to look completlely uncorrelated (just like a random signal).

- The following was changed: change fft($\theta$) to fourier($\theta$) ( function *fourier2.m* )

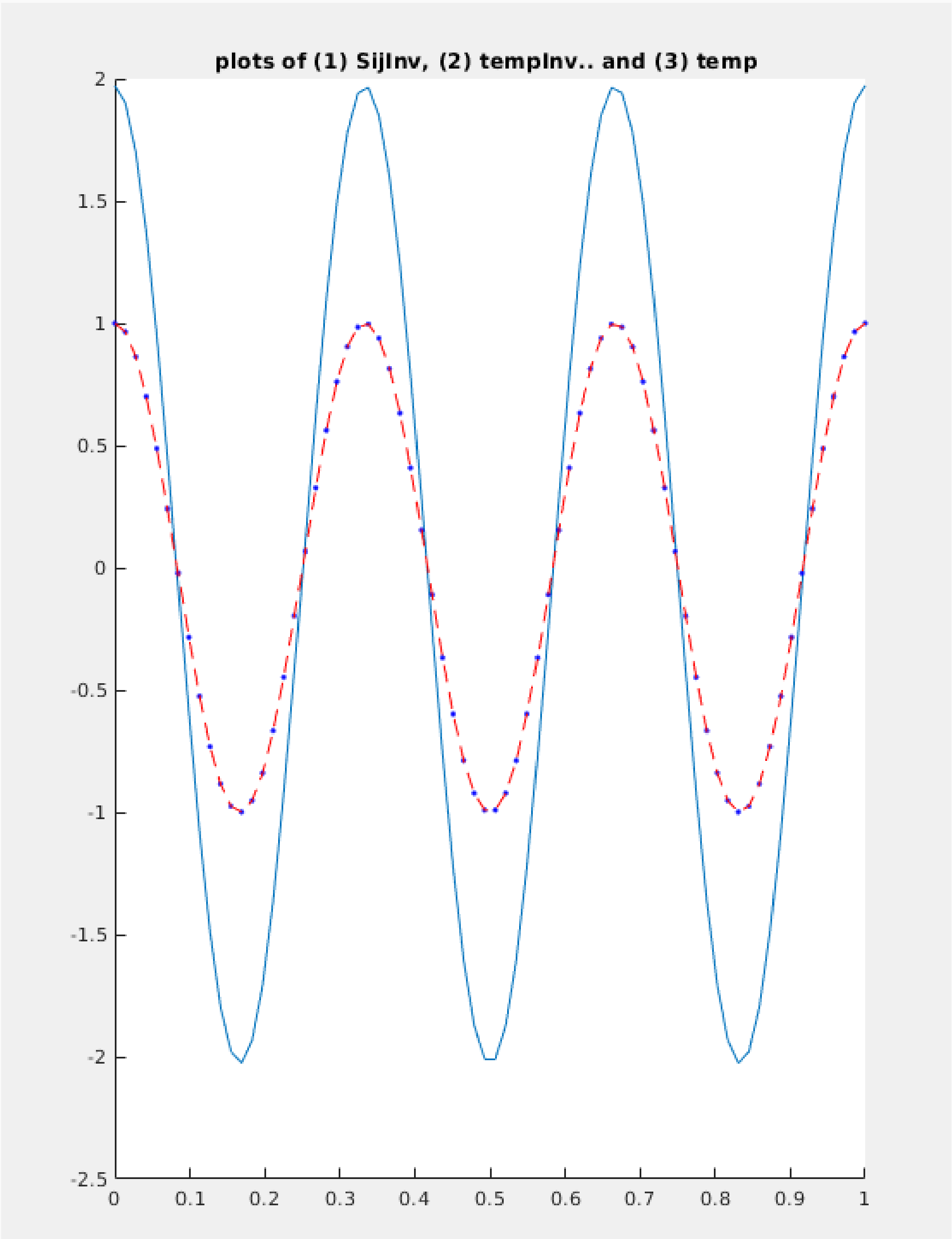


**Figure 24: Shown:** (1) original curve (blue dots) with reconstructed fourier approximation (red line); solid blue is real part of fourier coefficient.

**Definition (Full Procedure for Master Branch *<2022-05-27 Fri>*)**

- Spectral procedure follows Smits 2017.
- Pod procedure follows Smits 2017.

- Part 1. Spectral Analysis
  - Step A. take fft azimuthally
    - use half of $\theta$ data to avoid aliasing
    - Note: in my opinion $\sum_{m=0}^{M}(fft(theta))\,(cos(\theta)+i*sin(\theta))$ rather than just the fft ought to be used. This is done in (cite).
    - #TODO: include this in next update
  - Step B. find correlation in $t'$ described in Smits2017.below.eq.2.4.

$$\mathsf{R}\left(km;t,t'\right)=\frac{1}{T}\int_{r}\mathsf{u}(k;m;r,t)\mathsf{u}^{*}\left(k;m;r,t'\right)r\,\mathrm{d}r\equiv\left\langle \mathsf{u}(k;m;r,t)\mathsf{u}^{*}\left(k;m;r,t'\right)\right\rangle_{r} \tag{6}$$

- Create this option: use of function xcorr used/not used
  - currently: (when function m5.m on master branch *<2022-05-27 Fri>* is used) — the above equation for $R$ done as a explicitly as $\int uu^{*}$.

- Note that in the standard textbook case, we are correlating spatially and forming the ensemble time average. In anticipating the snapshot POD, the opposite is done: temporal correlation is found, and then the weighted (with $r$) spatial average (via integration) is found.

- Step C. take fft in $x$ of th above correlation to get $k$ modes.

- Part 2. Snapshot POD
  - the crossspectra for the kernal of the pod is given by the $r$ -averaged function

$$\lim_{\tau\to\infty}\frac{1}{\tau}\int_{0}^{\tau}\mathsf{R}\left(k;m;t,t'\right)\alpha^{(n)}\left(k;m;t'\right)\mathrm{d}t'=\lambda^{(n)}(k;m)\alpha^{(n)}(k;m;t) \tag{2}$$

- Note that $\alpha^{(n)}$ act as the eigenfunctions in the above Second Type Fredholm integral equation. This is simply the formulation of the snapshot POD.
- Step D. Find the (sorted) eigenvalues $\alpha^{(n)}$ found in (2) to solve for $\Phi^{(n)}$,

$$\lim_{\tau\to\infty}\frac{1}{\tau}\int_{0}^{\tau}\mathsf{u}_{\mathrm{T}}(k;m;r,t)\alpha^{(n)^{*}}(k;m;t)\mathrm{d}t=\Phi_{\mathrm{T}}^{(n)}(k;m;r)\lambda^{(n)}(k;m)$$

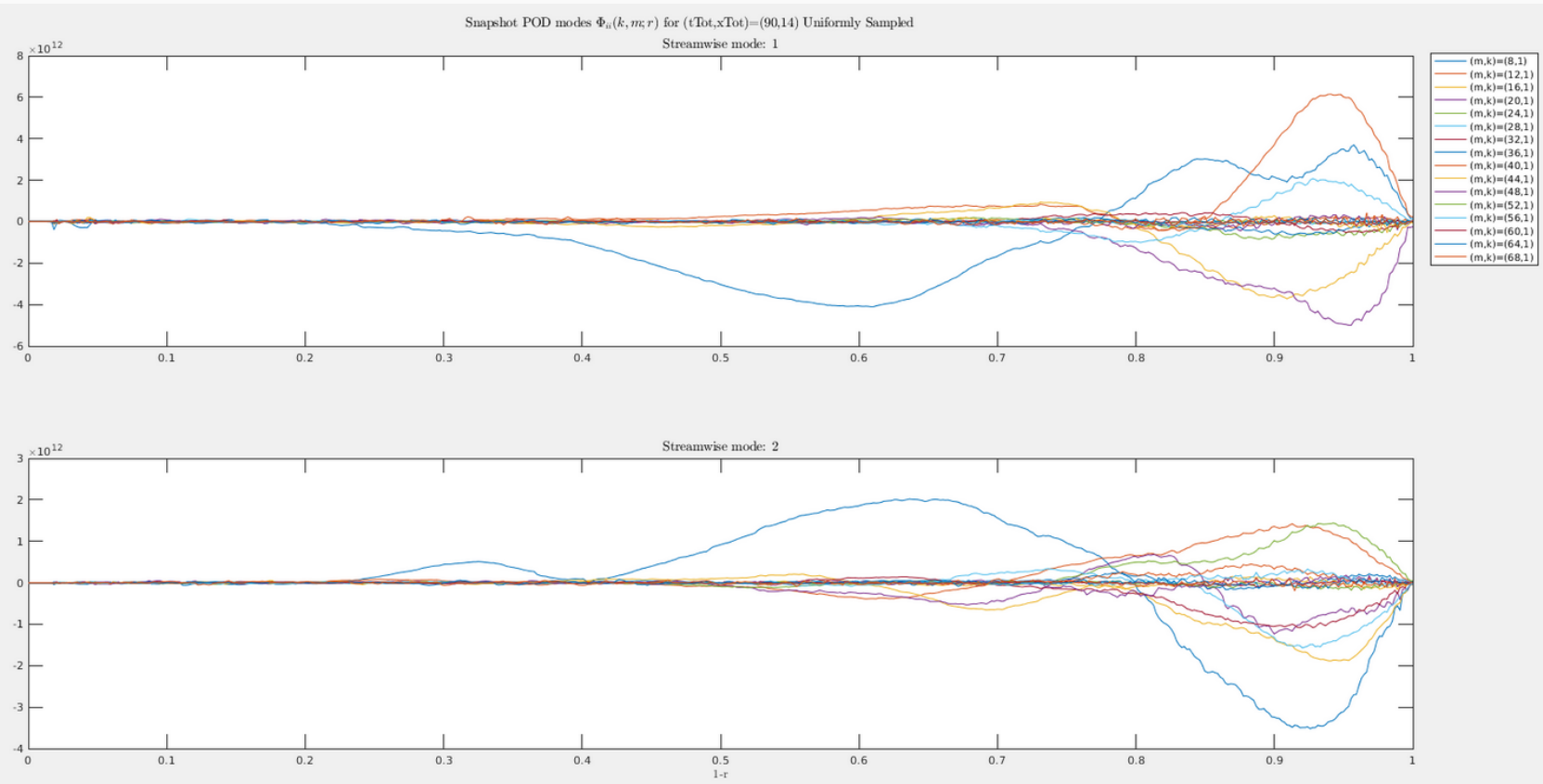


**Figure 25:** Shows snapshot POD for differen $k$ modes; the timestep and crosssection data is uniformly spaced, with 90 timesteps and 14 crossections used. The small data sample is shown since this code branch must be parallized (in next update). **Note also**, that Smits2017 averages all $k$ -mode graphs.

- Issues and Guiding Principles.
  - #TODO: Unfortunatelty, the maximum value is not occuring along the diagonal., as should occur with correlation coefficient matrices (!)
  - The matrix is positive semidefinite however (positive $\sqrt{\sigma_i} > 0 \forall i$.)
  - As alternative to $uu^H$ calculation, suggest using
    1. xcorr() so: $xcorr(u, u^H)$ and form the symmetric matrix with zero lag along the diagonal. Make sure xcorr correctly conjugates the complex part.
  - Alternately use $corrcoef(u, u^H)$. The good point with this is the diagnonal entries are 1 automatically.
  - Value of $r$. $r \in [0, 0.5]$. That seems to be equallly spaced (but check that).
    - see file `file:///mnt/archLv/mike/podTimeCoeffCopy/tests/run/fftCode/snapWithXYonly.dat`
    - The value of $dr = \ldots$ ; presumable dr $\approx$ 0.5/540$.

- Example correlation coefficient matrix $R$.
  - The maximum values should occur along the diagonal since this is 0 lag occurs (but do not have that)
  - Here is the integrated correlation tensor with the $\int ruu^* \, dr$ minimalbeispiel,

$$\mathbf{R}\left(x_1, m_1; t, t'\right) = \begin{bmatrix} -1.9672 & -3.3689 & -3.6159 & -2.7419 & -2.5511 \\ -3.3689 & -5.7692 & -6.1922 & -4.6955 & -4.3688 \\ -3.6159 & -6.1922 & -6.6463 & -5.0398 & -4.6891 \\ -2.7419 & -4.6955 & -5.0398 & -3.8216 & -3.5557 \\ -2.5511 & -4.3688 & -4.6891 & -3.5557 & -3.3083 \end{bmatrix} \quad \text{, ntimesteps} = 5 \tag{7}$$

which is indeed symmetric. This is matlabcorrMatSmits(1).dat.

- Intermediate Results
- Intermediate Spectral Results Graphs
  - Check if correlation matrix is formed properly. Sometimes (depending on how they were obtained), it turns out that the set of correlations doesn't form a proper correlation matrix. One way to check whether you do is to take the singular value decomposition and check all the singular values are non-negative.

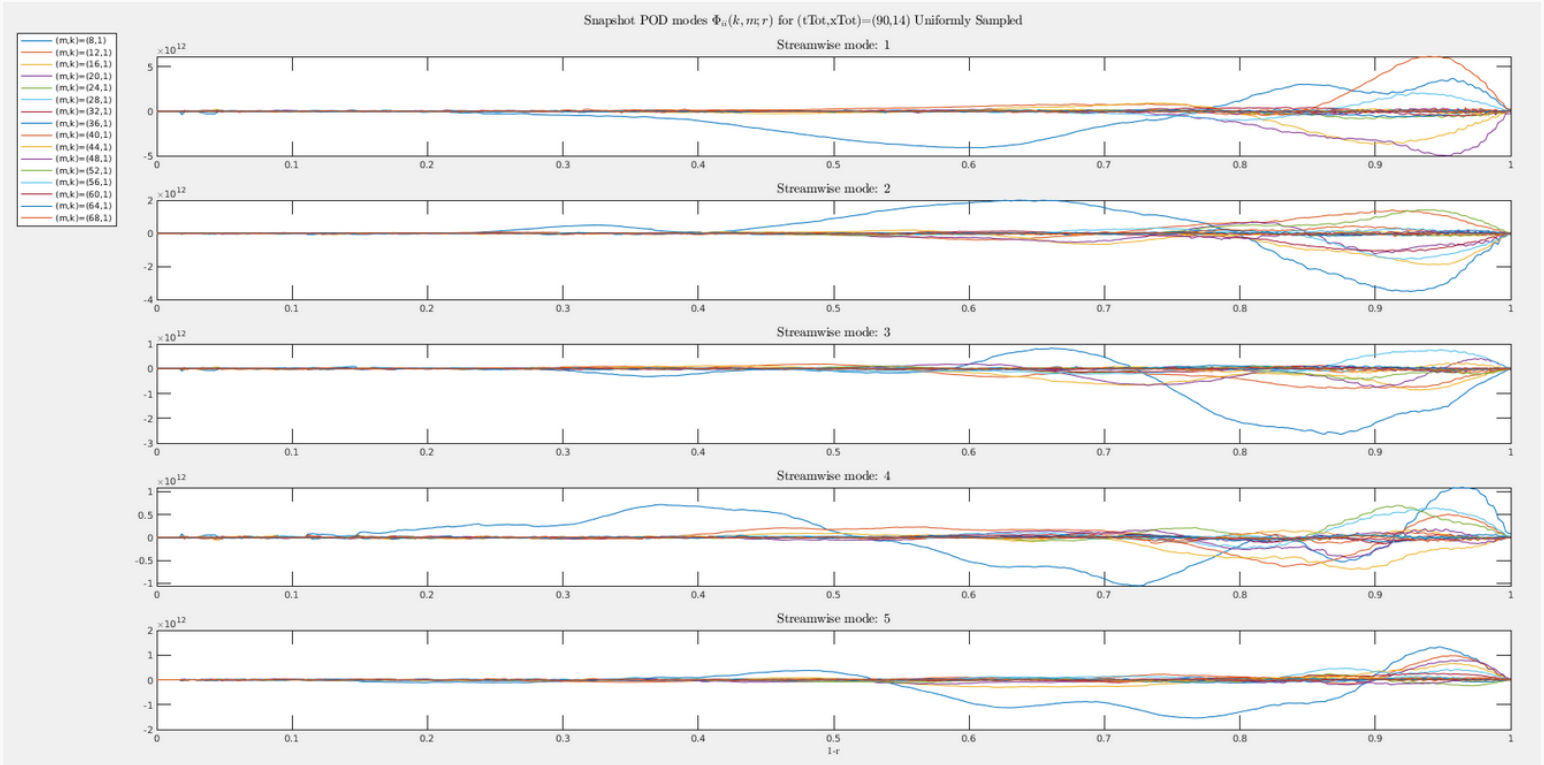


**Figure 26:** Shows snapshot POD for 5 differen $k$ modes (5 shown, total is 14); These need to be averaged